

Measuring Speed of Sound and Thermal Diffusivity in the Diamond Anvil Cell¹

E.H. Abramson^{2,4}, J. M. Brown³, L. J. Slutsky² and S. Wiryana²

¹ Paper presented at the Fourteenth Symposium on Thermophysical Properties,
June 25-30, 2000, Boulder, Colorado, U. S. A.

² Department of Chemistry, University of Washington, Seattle, Washington 98195,
U. S. A.

³ Department of Geophysics, University of Washington, Seattle, Washington 98195,
U. S. A.

⁴ To whom correspondence should be addressed.

ABSTRACT

Transient grating spectroscopy in the diamond-anvil high-pressure cell permits, in favorable cases, determination of the equation of state and thermal transport properties of fluids at high temperature and pressure. Measurements of the velocity of sound and thermodynamic properties of aqueous Na_2SO_4 to 3.4 GPa 300°C and the thermal diffusivity of oxygen are reported as examples of the application of this technique.

KEY WORDS: chemical potential, equation of state, high pressure, oxygen, sodium sulfate, thermal conductivity, thermal diffusivity, transient grating spectroscopy

1. INTRODUCTION

The thermodynamic properties and transport coefficients of simple fluids at high temperature and pressure play an important role in the earth [1] and planetary sciences [2]. These quantities also provide a necessary test of empirical potentials from which the equation of state and other kinetic and thermodynamic properties at experimentally difficult conditions might be deduced. Although there have been extensive studies of the properties of liquids in conventional piston-cylinder high-pressure systems the thermodynamic properties of liquids and solutions in much of the higher pressure portion of the pressure-temperature plane accessible in the diamond-anvil cell are not conveniently investigated. Similarly, experimental study of transport at high pressure has proven to be difficult. The thermal diffusivity of liquid water has been reported only at

pressures below 0.8 GPa [3] although water and aqueous mixtures are principal detonation products, and the properties of water at much higher pressures are important in geophysical and geochemical modelling [1]. Measurements for the diatomic gases by traditional techniques have not been extended beyond 1.0 GPa [4].

Transient Grating Spectroscopy [5, 6] permits the determination of both the thermal diffusivity and the velocity of sound in the heated, diamond-anvil cell [7, 8]. From the pressure and temperature dependence of the velocity the equation of state of a fluid can be deduced. Thus in a solution the pressure dependence of the chemical potential of a solute species can be calculated. Examples are given here from studies of aqueous Na_2SO_4 and fluid oxygen extending to temperatures of 300°C and to pressures of 3.4 and 13 GPa, respectively.

2. VELOCITY OF SOUND

In the experiments reported here two successive "excitation" pulses, 80 ps in duration, selected from the output train of a Q-switched, mode-locked, Nd:YAG laser are recombined in the sample at an angle 2θ , but otherwise coincident in space and time. Interference establishes a periodic distribution of intensity. In a sample that absorbs at the wavelength of the laser light, $\lambda_{IR}=1.064\mu\text{m}$, a (spatially) periodic variation in the temperature ensues. The associated thermal pressure launches counterpropagating acoustic waves. The acoustic wavelength, λ_A , expressed in terms of λ_{IR} and θ is

$$d = \lambda_A = \frac{\lambda_{IR}}{2\sin \theta} \quad (1)$$

The impulsively excited acoustic waves induce a temporally and spatially periodic variation in the index of refraction of the sample. A third pulse selected from the same Q-switched envelope as the excitation pulses is doubled to 532 nm and delayed by time of flight to generate the probe. Observation of the intensity of the Bragg scattering of the probe by the acoustic grating as a function of probe delay serves to determine the frequency (f_A), and hence the velocity ($c = \lambda_A f_A$), as well as the attenuation of the acoustic waves.

A representative time-domain record for 0.5 molal aqueous Na_2SO_4 at 89°C and 1.82 GPa in an inconel-gasketed diamond anvil cell is given in Fig.1. The apparent decay of the acoustic modulation here stems from purely geometric attenuation as the acoustic disturbance propagates beyond the volume illuminated by the probe (the separation of geometric attenuation from absorption is discussed in Ref. 7) and no dispersion that might be indicative of slow chemical or structural relaxation is observed.

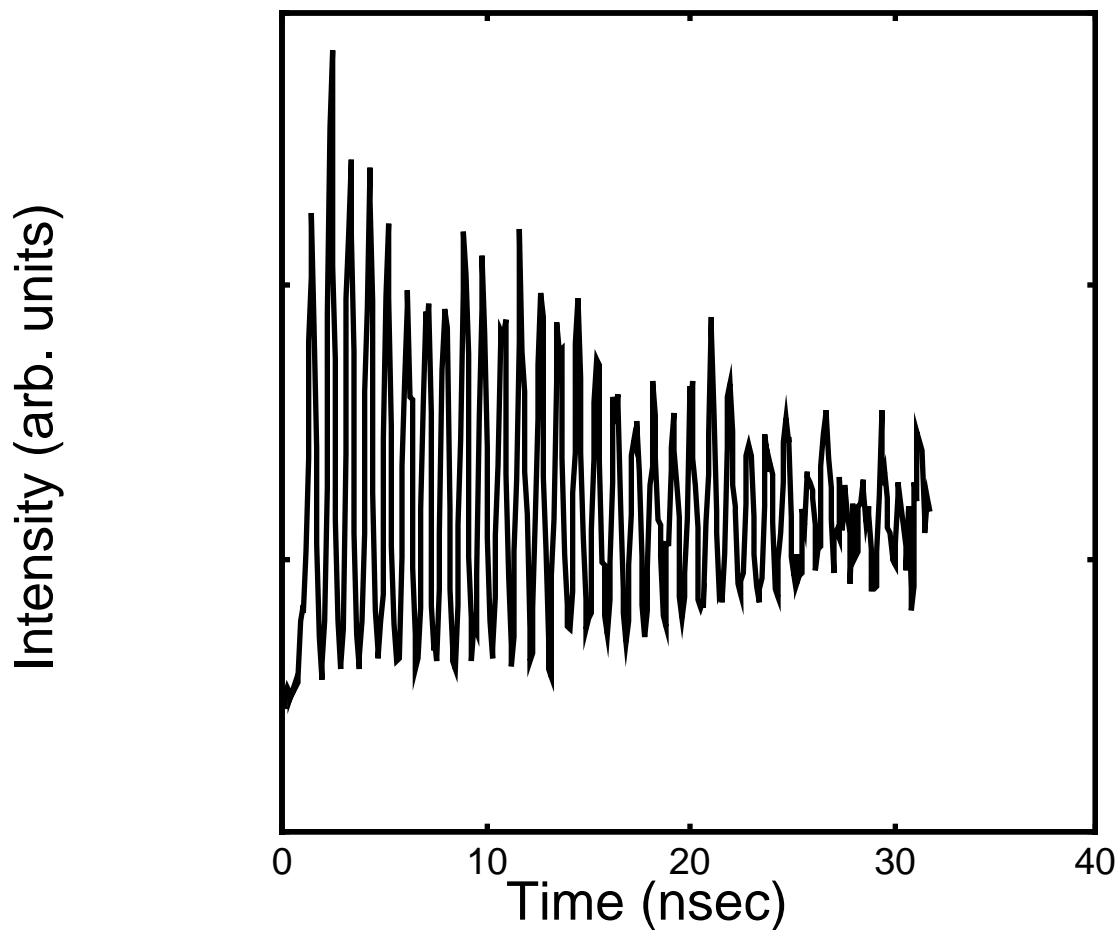


Fig. 1. The scattered intensity as a function of probe delay in 0.5 molal Na_2SO_4 at 89°C and 1.82 GPa. The frequency is 1.0735 GHz, the wavelength $3.011\ \mu\text{m}$ corresponding to an angle of intersection of 20° .

Velocities in aqueous Na_2SO_4 have been measured as functions of temperature, pressure, and composition both in a Merrill-Basset diamond-anvil cell and at pressures below 0.03 GPa also in a conventional cell fabricated from Inconel 625 with optical access

through sapphire windows. Data at pressures up to 0.03 GPa are displayed in Fig. 2, Results to 3.4 GPa in the diamond-anvil cell are given in Fig. 3 and in Table I.

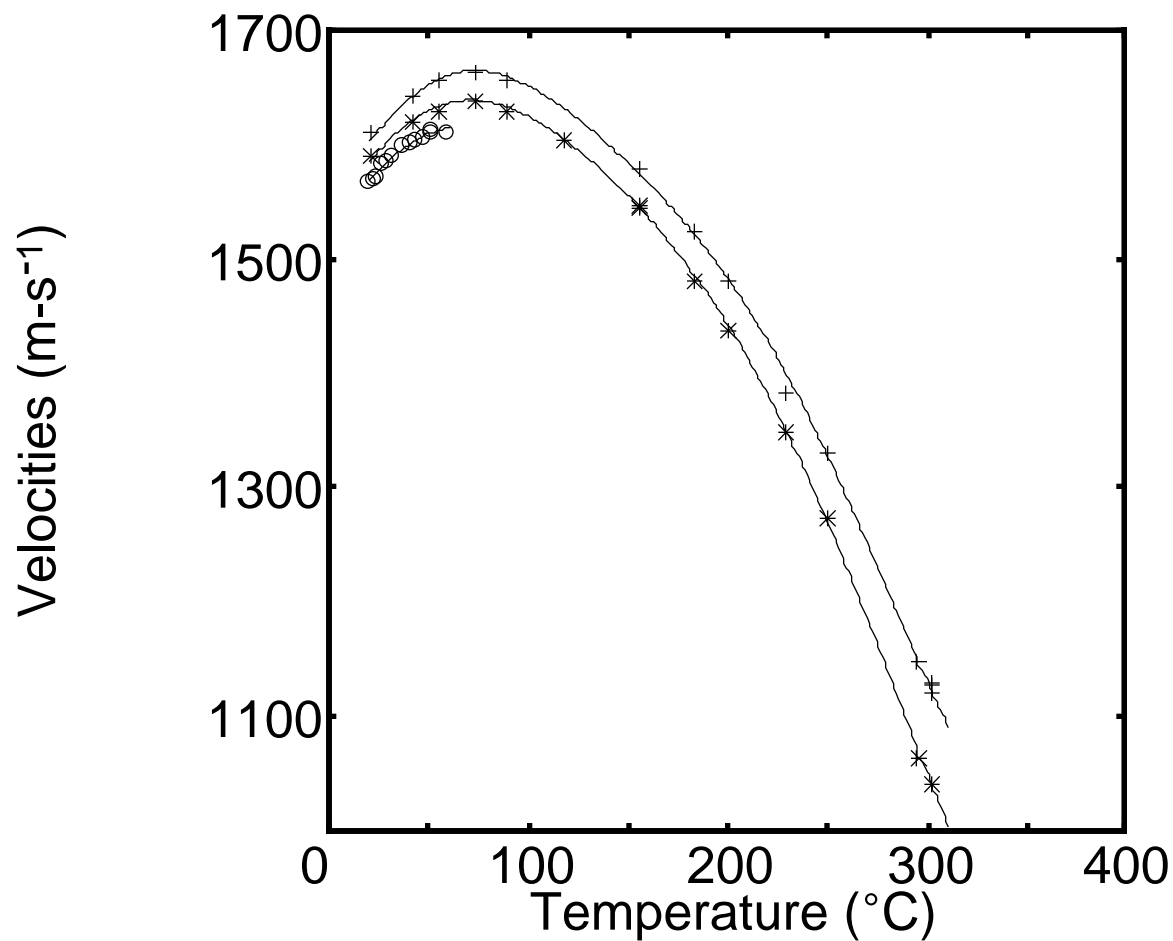


Fig. 2. The velocity of sound in 0.5 molal Na_2SO_4 at representative pressures between 1 bar and 276 bar and temperatures between 20°C and 300°C. The symbol (o) represents data at 1 bar, (*) data at 138 bar and (+) results at 276 bar.

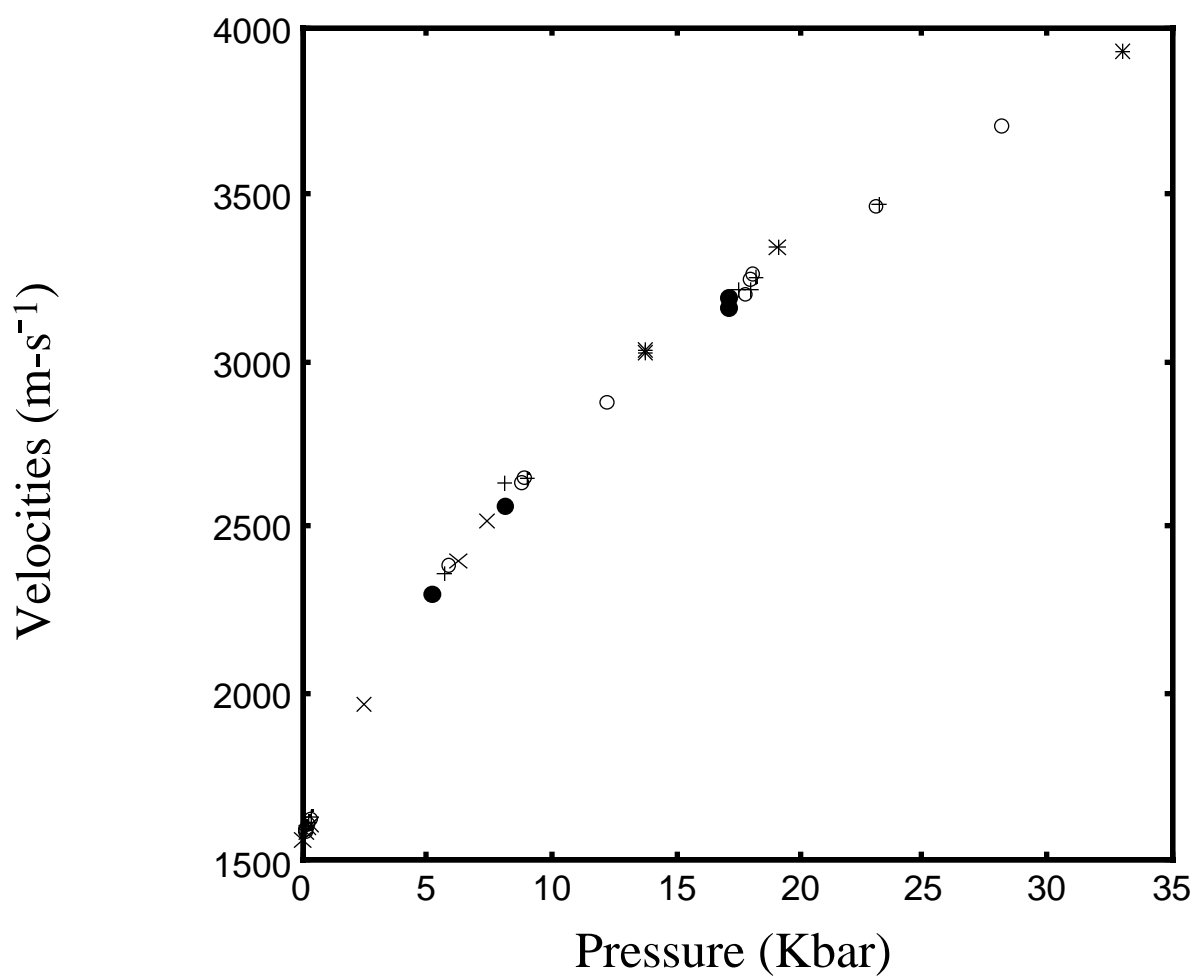


Fig. 3. Velocity of sound in 0.5 molal aqueous Na_2SO_4 as functions of temperature and pressure. Data at 20°C are represented by (x), data at 89°C by (filled circles), data at 117°C by (+), data at 130°C by (o), and data at 200°C by (*). Pressures in the diamond-anvil cell are measured by ruby fluorescence [9-11].

At temperatures where the density and heat capacity of a fluid or solution are known at least one point on an isotherm, the equation of state at fixed composition can be determined by recursive integration of

$$\frac{\rho}{P_T} = \frac{1}{c^2} + \frac{T\alpha^2}{c_p} \text{ and } \frac{c_p}{P_T} = -T \frac{v_{sp}^2}{T^2} \quad (2)$$

where ρ is the density, α the coefficient of thermal expansion, c_p the specific heat and v_{sp} the specific volume. To deduce v_{sp} at higher temperatures, the Gibbs free energy per gram at each composition is expanded about a convenient temperature and pressure in the form

$$G_{sp} = \sum_{ij} A_{ij} P^i T^j \quad (3)$$

appropriately differentiated and the coefficients adjusted to match the P , v_{sp} , T relations and the pressure-dependence and temperature-dependence of the heat capacity, where known in addition to the measured velocity of sound at high temperature and pressure. The continuous curves in Figure 2 represent the result of this latter procedure, (with indices i and j running from 0 to 4) applied to 0.5 molal Na_2SO_4 at pressures up to 0.03 GPa and temperatures to 300°C. The specific volume is then

$$v_{sp} = \frac{G_{sp}}{P_T} \quad (4)$$

If f is the fraction by weight of solute in a binary mixture, the quantity $(v_{sp}/1-f)$ is the volume of the solution that contains 1 gram of solvent. The number of moles (n) of a

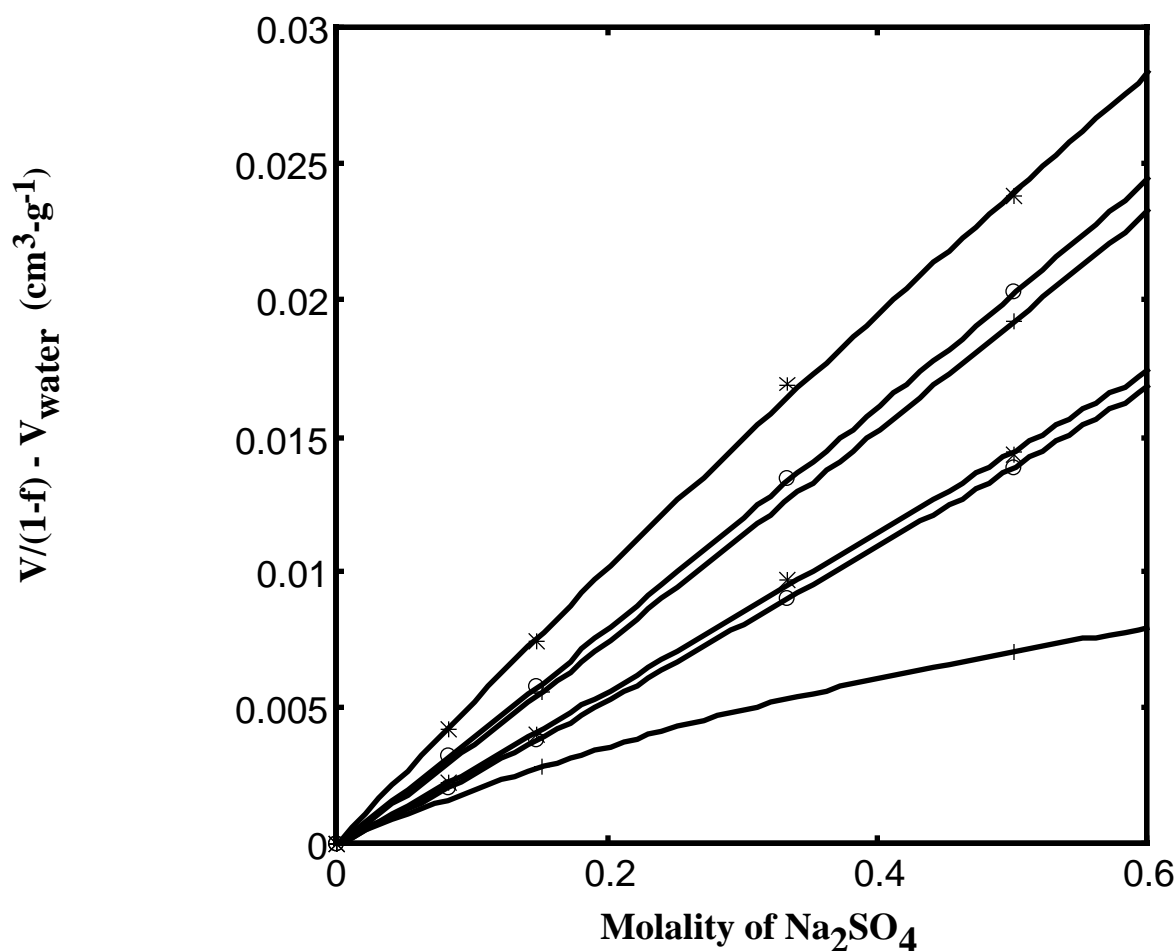


Fig. 4. The effect of temperature and pressure on the specific volume of aqueous sodium sulphate at higher pressures. The quantity y at 0.1 GPa (lower three curves) and 0.5 GPa (upper three curves) is plotted versus molality at 25°C (*), 100°C (o), and 200°C(+).

solute species with formula weight w in this volume is then $n = f/(1-f)w$. It is convenient to introduce the definition $y = (v_{sp}/1-f) - v^\circ$ where v° is the specific volume of the pure solvent. Differentiation of y with respect to n gives the partial molal volume of the solute,

\bar{V} , Integration of

$$\frac{\mu}{P_{TP}} = \bar{V} \quad (5)$$

then yields the pressure dependence of μ , the chemical potential of the solute species at any composition. A representative plot of y against n is given in Fig. 4 where the initial slope determines the pressure derivative of the standard chemical potential, the deviation from linearity the pressure dependence of the excess free energy.

3. THERMAL DIFFUSIVITY

When the acoustic disturbance has been fully damped, a spatially periodic distribution of temperature and hence index of refraction remains. This grating decays exponentially by thermal diffusion with a characteristic time, τ , given by $\tau^{-1} = 4\pi^2 D d^{-2}$ where D is the thermal diffusivity (the thermal conductivity divided by the heat capacity per unit volume) of the fluid. The variation of τ with d serves to distinguish thermal diffusion from other relaxation processes and at high temperature permits a straightforward separation of non-diffusive radiative transport from diffusive processes. Given the long thermal relaxation times characteristic of molecular fluids, in the case of a strong signal, a continuous (argon ion) laser may be substituted for the pulsed probe and the signal be captured with a transient recorder over the full duration of the decay, for each pulse of the excitation laser. Semi-log plots of such data are given in Fig. 5 for oxygen in the diamond-anvil cell at 300°C and 12.7 GPa, as well as for water and methanol under ambient conditions.

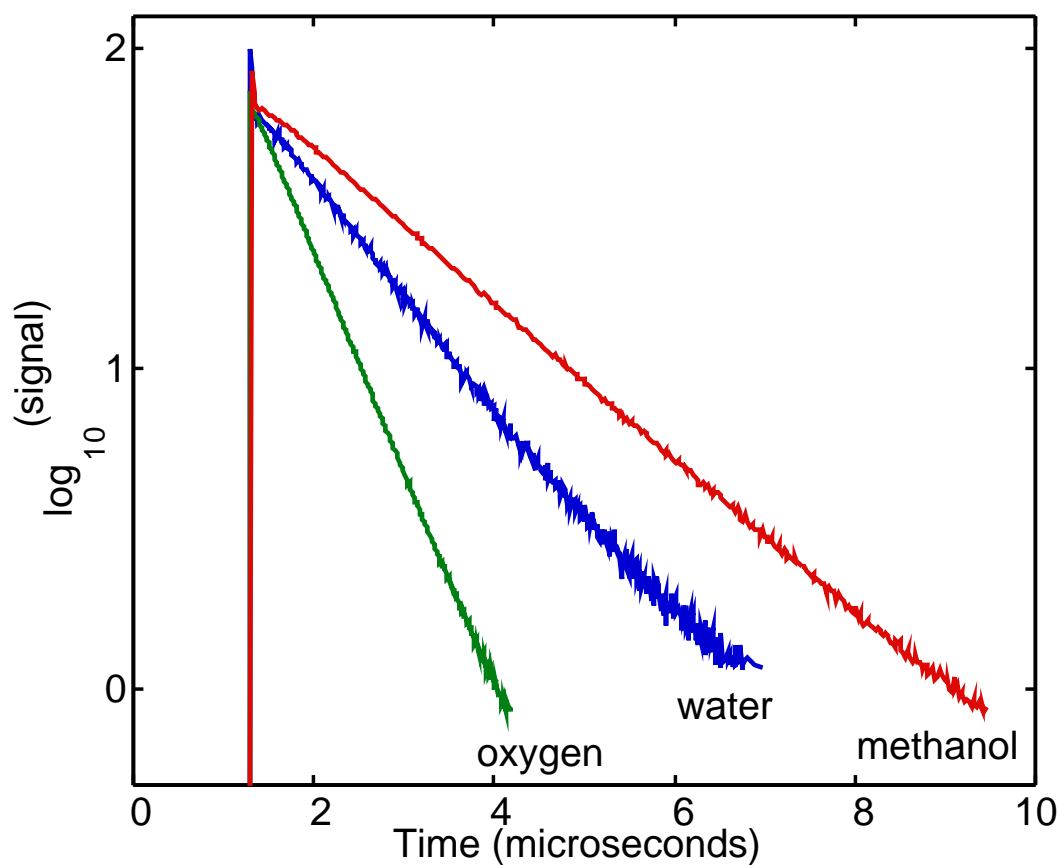


Fig. 5. Semi-logarithmic plots of the Bragg-scattered intensity from oxygen in the diamond-anvil cell (12.7 GPa, 300°C), as well as water and methanol at ambient conditions.

4. DISCUSSION

Sodium sulfate was selected for preliminary studies both as a representative and relatively unreactive electrolyte and as a postulated major constituent of "Europa's briny deep" [18]. The determination of the specific volume at higher pressures by integration of Eqs. 2 is based, up to 150°C, on experimental values at ambient pressure or along the

coexistence curve [19, 20]. Specific volume as a function of pressure, temperature and concentration is given in Tab. II.

The acoustic velocities that are the principal determinants of the change in density with respect to pressure are measured to 0.2 %. It is likely that below 150°C, the errors in the specific volumes in Tab. II are not much larger than the errors in the initial densities, in particular in the values at temperatures above 100°C along the coexistence curve. At the higher pressures explored in the diamond anvil cell the pressure derivative of the velocity is roughly $1000 \text{ m}\cdot\text{s}^{-1}\cdot\text{GPa}^{-1}$. Random velocity errors of approximately $\pm 30 \text{ m}\cdot\text{s}^{-1}$, consequent upon errors in the measurement of pressure, must be expected. This is consistent with the departures from smooth variation of the velocity with temperature and pressure exhibited by the data in Tab. I. A systematic error of 0.1 % in the velocity would contribute an error of 0.08 % in the specific volume at 3.5 GPa and an error of $2 \text{ cm}^3\cdot\text{mole}^{-1}$ in the apparent partial molal volume in a 0.5 molal solution.

The partial molar volume of Na_2SO_4 at infinite dilution is given as a function of temperature and pressure in Table III. At high temperature and low pressure the large negative electrostrictive contribution predominates. Indeed, below 0.3 kbar the pressure and temperature dependence of V° can be calculated from the temperature and pressure dependence of the dielectric constant of water [21]. The increase in V° with P at pressures above 0.1 GPa cannot however be interpreted as principally due a decrease in the magnitude of the negative electrostrictive term.

The thermal diffusivities of fluid oxygen have been measured to pressures of over 12 GPa and temperatures from 25 to 300°C; results are discussed in Ref. 22. Typically,

measurements have been made with the use of a continuous, probe laser to an accuracy of 2%. Oxygen provides a particularly large signal due to a resonant electronic transition at the fundamental frequency of our Nd:YAG laser. At elevated pressures most other materials, in particular water, yield smaller signals, which necessitates the use of a pulsed probe; the accuracy of the results should be comparable.

ACKNOWLEDGEMENTS

This work was supported by Grant Nos. EAR 96-14313 and EAR 98-14599 from the National Science Foundation and by research subcontract B5030002 from Lawrence Livermore National Laboratory.

REFERENCES

1. T. J. Ahrens, *Nature* **342**: 122 (1989)., J. M. Delaney and H. C. Helgeson. *Am. J. Sci.* **278**: 638 (1978).
2. D. J. Stevenson and E. E. Salpeter. *Astrophys. J. Suppl.* **35**: 221 (1977).
3. A. W. Lawson, E. Lowell and A. L. Jain, *J. Chem. Phys.* **30**: 643 (1959).
4. B. Le Neindre, Y. Garrabos and R. Tufa, *Physica A.* **156**: 512 (1989).
5. M. D. Fayer, *Annu. Rev. Phys. Chem.* **33**: 63 (1987)
6. Y. X. Yan, L. T. Cheng, and K. A. Nelson, in *Advances in Non-linear spectroscopy*, J. H. Clark and R. E. Hester, Eds. (John Wiley Ltd. London, 1987)
7. J. Zaug, L. J. Slutsky, and J. M. Brown, *J. Phys. Chem.* **98**: 6008 (1994)
8. J. Zaug, E. H. Abramson, J. M. Brown, and L. J. Slutsky, in *High Pressure Research; Applications to Earth and Planetary Sciences*, Y. Syono and M. Manghnani, Eds. (American Geophysical Union, Washington D. C., 1992), p.157
9. H. K. Mao, P. M. Bell, J. W. Shaner, and D. J. Steinberg, *J. Appl. Phys.* **49**: 3276 (1978)
10. G. J. Piermarini, S. Block, and J. D. Barnett, *J. Appl. Phys.* **44**: 5377 (1973)
11. S. C. Schmidt, D. Shiferl, A. S. Zinn, D. D. Ragan, and D. S. Moore, *J. Appl. Phys.* **69**: 2793 (1991).
12. S. L. Wunder and P. E. Schoen, *J. Appl. Phys.* **52**: 3772 (1981).
13. R. Vedam and G. Holton, *J. Acoust. Soc. Am.* **43**: 108-116 (1968).
14. T. Grindley and J. E. Lind Jr., *J. Chem. Phys.* **54**: 3983 (1971).

15. A. Saul and W. Wagner, *J.Phys.Chem. Ref. Data* **18**: 1537 (1989), *ibid* **17**: 1439 (1988).
16. E. H. Abramson, L. J. Slutsky, M. D. Harrell and J. M. Brown, *J. Chem. Phys.* **110**: 10493 (1999).
17. W. A. Wakeham in *Transport Properties of Fluids*, edited by J. Millat, J. H. Dymond and C. A. Nieto de Castro (Cambridge University Press, Cambridge, 1996).
18. J. S. Kargel, *Icarus* **94**: 368-390 (1991), *Science* **280**: 1211 (1998).
19. P. S.Z. Rogers and K. S. Pitzer, *J. Phys. Chem.* **85**: 2886 , (1981).
20. A. Korosi and B. M. Fabuss, *J. Chem Eng. Data* **13**: 548 (1968). C. D. Synowietz, J. Dans, and H. Surawski, Densities of Binary Aqueous Systems and Heat Capacities of Liquid Systems. IV(macroscopic and technical properties of matter.). Numerical Data and Functional Relationships in Science and Technology, Landolt Bornstein, Zahlenwerte und Funktionen, Band II, Teil 1, Springer, Berlin (1971)
21. E. H. Abramson, J. M. Brown and L. J. Slutsky, *Annu. Rev. Phys. Chem.* **50**: 279 (1999)
22. E. H. Abramson, L. J. Slutsky and J. M. Brown, *J. Chem. Phys.* **111**: 9357 (1999)

Table I. Locally interpolated velocities of sound ($\text{m}\cdot\text{sec}^{-1}$) in aqueous 0.5 molal Na_2SO_4 as a function of temperature and pressure

[illegible]

Table II. Specific volume ($\text{cm}^3\text{-gm}^{-1}$) of 0.5 molal and 0.148 molal aqueous Na_2SO_4 as a function of temperature and pressure

m	0.500	0.500	0.500	0.500	0.148	0.148	0.148	0.148
P (kbar)	25.°C	100.°C	130°C	200°C	25°C	100°C	130°C	200°C
0.001	0.9454	0.9832			0.9844	1.0240		
0.270	0.9358	0.9723	0.9934	1.0573	0.9734	1.0117	1.0345	1.1110
1.00	0.9131	0.9468	0.9652	1.0175	0.9476	0.9833	1.0026	1.0628
2.00	0.8876	0.9188	0.9348	0.9774	0.9189	0.9532	0.9687	1.0165
4.00	0.8494	0.8764	0.8901	0.9227	0.8766	0.9064	0.9195	0.9554
6.00	0.8213	0.8448	0.8571	0.8850			0.8834	0.9135
8.00		0.8198	0.8311	0.8559			0.8560	0.8819
10.00			0.8096	0.8320			0.8332	0.8564
12.00		0.7819	0.7913	0.8119			0.8141	0.8349
14.00		0.7667	0.7753	0.7946			0.7977	0.8165
16.00		0.7533	0.7612	0.7793			0.7832	0.8004
18.00			0.7485	0.7656			0.7704	0.7861
20.00			0.7371	0.7533			0.7589	0.7733
24.00			0.7173	0.7315			0.7388	0.7510
28.00			0.7005	0.7129			0.7217	0.7322
34.00				0.6896				0.7085

Table III . Partial molal volumes of Na_2SO_4 at infinite dilution as a function of temperature and pressure ($\text{cm}^3\text{-mole}^{-1}$)

P(kbar)	0.001	0.068	0.160	0.270	1.0	2.0	3.0	5.0	8.0	16.0	24.0
25°C	12.1	13.8	15.2	16.6	24.7	33.0	40.4	50.5			
50°C	13.4	14.5	15.7	16.8	24.9	31.2	36.4	44.3	52.9		
100°C	10.3	11.4	12.8	14.2	21.9	27.0	31.0	37.3	44.7	58.9	
130°C		1.3	2.9	4.5	15.0	23.8	30.4	38.4	49.4		
150°C		-6.3	-4.2	-1.5							
190°C		-34.6	-30.3	-25.5							
200°C		-41.8	-36.2	-30.9	11.6	22.4	27.6	33.8	37.8	46.1	59.0
230°C		-79.2	-69.5	-59.8							
250°C		-120	-104	-89.1							